ADBA Chaos and Fractals
Cutting-Edge Scientific Solutions

e-ISSN: 3023-8951
RESEARCH ARTICLE
Vol.2 / No.1 / 2025 / pp.14-19
https://doi.org/10.69882/adba.chf.2025013

Permanent Magnet Synchronous Motor with Load Torque: Dynamics, Circuitry Execution and Control

Rolande Tsapla Fotsa[*,1], **Paloma Kevina Koubeu Papemsi**[α,2], **Gideon Pagnol Ayemtsa Kuete**[β,γ,3], **Justin Roger Mboupda Pone**[γ,4], **Serge Raoul Dzonde Naoussi**[Γ,5], **Foutse Momo**[ς,6] **and Pierre Ele**[ψ,7]

[*]Department of Mechanical Engineering, College of Technology, University of Buea, P.O. BOX 63 Buea, Cameroon, [α]Rousseau Higher Institute, University of Douala, P.O. Box 2701, Douala, Cameroon, [β]Laboratory of Energy and Electrical and Electronic Systems, Department of Physics, Faculty of Science, University of Yaounde I, P.O. Box 812, Yaounde, Cameroon, [γ]Research Unit of Automation and Applied Computer (RU-AIA), Electrical Engineering Department of IUT-FV, University of Dschang, P.O. Box: 134, Bandjoun, Cameroon, [Γ]Technology and Applied Sciences Laboratory (TASL), University Institute of Technology of Douala (IUT of Douala), University of Douala, Post Box 8698, Douala, Cameroon, [ς]Biomedical Engineering, Energy and Modeling Laboratory (BEEMo.Lab.), Higher Institute of Science and Technology (HIST), University of Mountains, P.O. Box 208, Bangangte, Cameroon, [ψ]Electrical and Engineering, Telecommunications Department, National Advanced School of Engineering, University of Yaounde I, P.O. Box 812, Yaounde, Cameroon.

ABSTRACT This paper is interested in the study of the dynamics and control of the permanent magnet synchronous motor with load torque (PMSMLT). PMSMLT has three fixed points where one is saddle and the two others are saddle focus. PMSMLT exhibits no oscillations, periodic characteristics, chaotic characteristics and coexistence between no oscillations and chaotic characteristics. In order to validate the results obtained numerically, an electronic implementation of PMSMLT is performed in probe simulation program with integrated circuit emphases (PSPICE) environment which reveals a concordance between the numerical simulations and the experimental verifications. The coexisting characteristics is eliminated by the linear augmentation control method.

KEYWORDS
Permanent magnet synchronous motor
Load torque
Chaos
Coexisting characteristics
Linear augmentation control
Implementation circuit

INTRODUCTION

Rotating machines are electrical systems intended for the majority to control industrial systems linked to their mechanization (Wildi 2006; Chapman 2005; Santoso and Beaty 2018). These machines are classified into two main categories depending on their use. There are direct current machines and alternating current machines. Due to its relatively simple control, DC machines are increasingly used and considered as electric actuators for motorizing multiple engineering applications such as high-speed trains, elevators, drones, crushing mills, etc. (Fitzgerald *et al.* 1991; Wildi 2006; Borisavljevic 2013). The synchronous machine in most cases is used in three phases. It behaves as a reversible electromechanical energy converter. Thus, it can operate in motor mode or in generator mode depending on the voltage: In motor operation, the electrical energy provided by the source is transformed into mechanical energy and in generator or alternator operation, the mechanical energy is transformed into redirected electrical energy towards the source (Say and Taylor 1980; Hughes 2006; El-Sharkawi 2000). In generator operation, the synchronous motor can redirect the electrical energy. This application finds opportunities in wind turbines for the production of electricity, thanks to the possibility of providing reactive energy by modulating the excitation current. The synchronous machine in alternator operation can be used in power plants for the conversion of mechanical energy into electrical energy (Chau and Wang 2011; Machowski *et al.* 2012; Leine and Nijmeijer 2004).

The synchronous machine consists of a rotating part and a fixed part, the two separated by an air gap. The rotor, which is the rotating part of the synchronous machine, can consist of permanent magnets or consist of a winding powered by direct current and a magnetic circuit (electromagnet). Permanent magnet synchronous motors (PMSM) have advantages and applications in the automotive sector: lower inertia and weight than those with a wound rotor, improved efficiency thanks to the absence of consumption in the rotor, and reduced maintenance due to the

Manuscript received: 21 January 2025,
Revised: 28 January 2025,
Accepted: 29 January 2025.

[1]rtsapla@yahoo.com (**Corresponding author**)
[2]palilomapapemsi@gmail.com
[3]pagnolayimtsa@gmail.com
[4]mboupdapone00@gmail.com
[5]sdzonde@gmail.com
[6]mfoutse@yahoo.fr
[7]pierre.ele@univ-yaounde1.cm

absence of brooms (Iqbal and Singh 2019; Cheukem *et al.* 2020; Hua *et al.* 2022). Several works have already been carried out on PMSM. This work essentially focuses on the search for chaos in the machine and the control of undesirable dynamic states such as chaos (Donglian *et al.* 2005; Luo 2014; Luo *et al.* 2014). In the mathematical model of PMSMs proposed in the literature, the authors do not consider the saliency ratio, which is very low. However, it should be noted that a low saliency ratio has a negative impact on the machine in the sense that the power factor (which increases with the saliency ratio) of the electrical installation will be very low, thus resulting in a lower active power developed by the very weak motor, which favors a very high current which, from an economic point of view, generates losses for the user. Furthermore, we note that the work on PMSMs was carried out when they are empty, that is to say, the load torque is zero (Maeng and Choi 2013; Vadivel *et al.* 2023; Yamdjeu *et al.* 2024; Mao and Liu 2019; Du-Qu and Bo 2009).

In light of what was presented earlier, it appears that the literature still remains vague on the behavior of PMSMLT (TL $\neq 0$: continuous or discrete variable). It would therefore be interesting to fully study these motors in the presence of load torque because in reality, a motor is made to be used and therefore cause a movement. The objective of this paper is to study the dynamics of a PMSMLT in the presence of mechanical load torque and to carry out its control in order to make it operate in the manner desired by the user. To carry out this paper, it is structured into four sections. The first section presents the introduction. Section two is devoted to the dynamic analysis of PMSMLT and its electronic implementation. Section three presents the control of unwanted dynamic states. The paper ends with a conclusion in section 4.

THEORETICAL ANALYSIS OF PMSMLT AND ITS ELECTRONIC IMPLEMENTATION

The PMSMLT is described by the set of equations (Cheukem *et al.* 2020):

$$\frac{dx}{dt} = -x + yz, \tag{1a}$$

$$\frac{dy}{dt} = -y - xz + \gamma z, \tag{1b}$$

$$\frac{dz}{dt} = \sigma(y - z) + T_L, \tag{1c}$$

where x and y are the dimensionless direct and quadrature currents, respectively, z the angle speed, T_L the dimensionless load torque and σ, γ are the system parameters. System (1) is invariant under the coordinate transformation $(x, y, z)(x, -y, -z)$. The PMSMLT is dissipative because $\nabla V = \frac{\partial \dot{x}}{\partial x} + \frac{\partial \dot{y}}{\partial y} + \frac{\partial \dot{z}}{\partial z} = -(2 + \sigma)$. The fixed points of PMSMLT are obtained by solving the system of equation $\dot{x} = \dot{y} = \dot{z} = 0$ which gives

$$x = z\left(z - \frac{T_L}{\sigma}\right) \tag{2a}$$

$$y = \frac{T_L}{\sigma} + z \tag{2b}$$

$$\sigma z^3 - T_L z^2 - (\gamma - 1)\sigma z - T_L = 0 \tag{2c}$$

Equation 2c admits fixed points whose number varies depending on the values of the torque T_L and the parameter σ. Using a digital calculator as well as the fixed values of the parameters ($\sigma = 4.56$; $\gamma = 20$; $T_L = 6.5$), three fixed points are obtained:

$$\begin{aligned} E_1 &= (0.1132, -1.5009, -0.0754), \\ E_{2,3} &= (19.2762, \pm 3.7352, \pm 5.1606). \end{aligned} \tag{2}$$

The stability of the system for each fixed point is determined by the evaluation of the eigenvalues of the Jacobian matrix

$$J = \begin{bmatrix} -1 & z & y \\ -x & -1 & -x + \gamma \\ 0 & \sigma & -\sigma \end{bmatrix}. \tag{4}$$

The characteristic equation corresponding to the first fixed point E_1 obtained using $\det(J - \lambda I) = 0$ is given by:

$$\begin{aligned} \lambda^3 + (\sigma + 2)\lambda^2 + (2\sigma + 0.1132\sigma + \gamma\sigma + 1.0056)\lambda \\ + \sigma(0.7679 - \gamma) = 0. \end{aligned} \tag{5}$$

The eigenvalues, the fixed points $E_{1,2,3}$ are presented in Table 1. Table 1 reveals that the fixed point E_1 is a saddle while the fixed points $E_{2,3}$ are saddle focus.

Table 1 Eigenvalues of fixed points $E_{1,2,3}$.

Eigenvalues	E_1	$E_{2,3}$
λ_1	-0.9940	$-0.0586 + 5.7173i$
λ_2	6.9039	$-0.0586 + 5.7173i$
λ_3	-12.4698	-6.4420

Numerical analysis of PMSMLT

In order to know the influence of the load torque and other parameters on the dynamical behaviours of PMSMLT, the 2D largest Lyapunov exponent (LLE) are illustrated in Figure 1.

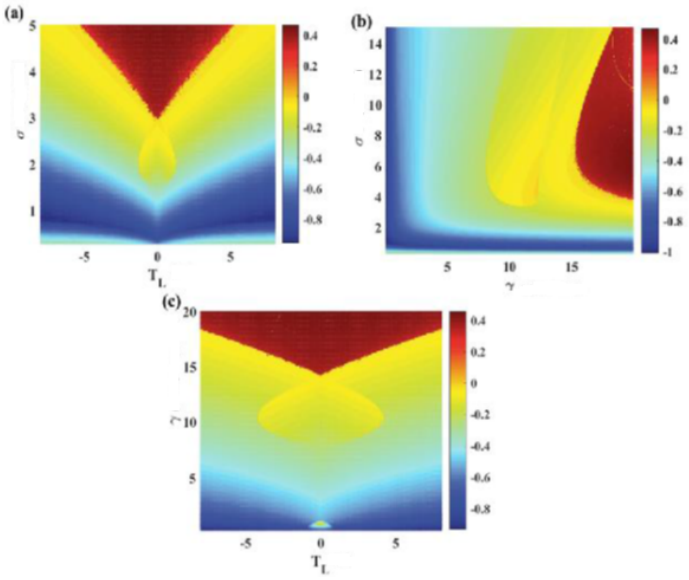

Figure 1 2D LLE in the planes: (a) (T_L, σ) with $\gamma = 20$, (b) (γ, σ) with $T_L = 2.0$, and (c) (T_L, γ) avec $\sigma = 8$ for the initial conditions $(x_0, y_0, z_0) = (0.01, 0.01, 0.01)$.

Figure 1 makes it possible to distinguish between chaotic zones (for positive LLE) and periodicity zones (for negative LLE) depending on the system parameters. Figure 2 represents the phase portrait of the chaotic state for fixed values of the system parameters.

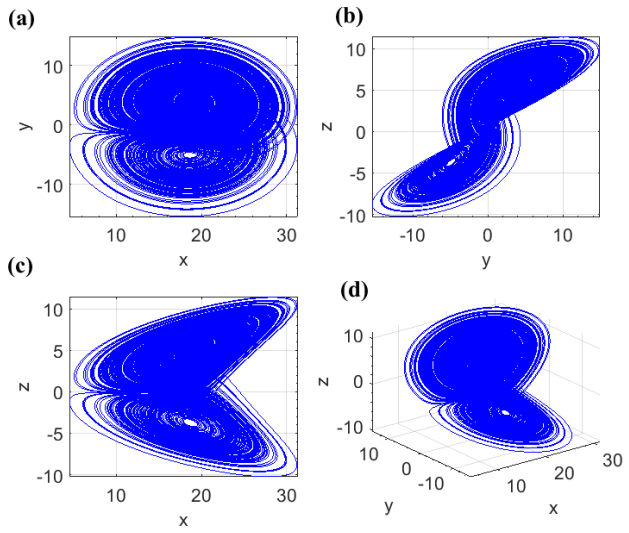

Figure 2 Phase portraits following the planes: (a) $(x$-$y)$, (b) $(y$-$z)$, (c) $(x$-$z)$, and (d) (x, y, z) for the following parameter values: $\sigma = 4.56$, $\gamma = 20$, $T_L = 6.5$ obtained for the initial conditions $(x_0, y_0, z_0) = (0.01, 0.01, 0.01)$.

Figure 2 shows the chaos encountered in the PMSMLT. Figure 3 presents the forward (in black) and return (in red) bifurcation diagrams of the PMSMLT forward current as well as their graphs of the corresponding LLE as a function of the T_L load torque.

The coexistence between chaos and no oscillations is observed in Figure 3 for the torque values between $6.448 \leq T_L \leq 5.824$ on the one hand and $5.824 \leq T_L \leq 6.448$ on the other hand. In order

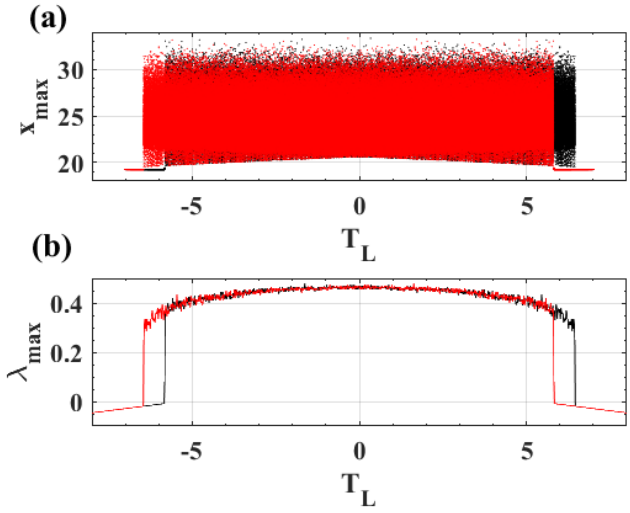

Figure 3 Bifurcation diagram showing the local maxima of x of the PMSMLT as a function of T_L load as well as the graph of the corresponding LLE for $\sigma = 4.56$ and $\gamma = 20$. The graphs in black represent the forward digraphs, and those in red represent the return.

to find the initial conditions leading to coexisting attractors, the drawing of the basin of attraction is carried out in Figure 4 by considering the parameter values leading to coexistence and the initial conditions are varied in the plane (x_0, y_0).

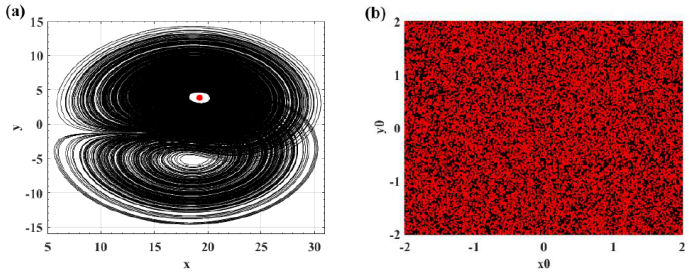

Figure 4 (a) Phase portrait in the plane (x, y) and (b) basin of attraction following the plane (x_0, y_0) putting for $\sigma = 5.46$, $\gamma = 20$, $T_L = 6.5$. The black lines are obtained using the initial conditions $(x_0, y_0, z_0) = (0, 0, 0)$, while the red lines are obtained using the initial conditions $(x_0, y_0, z_0) = (0, 0.2, 0)$.

Figure 4(a) shows the coexistence between chaos and the fixed point obtained respectively by the initial conditions $(x_0, y_0, z_0) = (0, 0, 0)$ and $(x_0, y_0, z_0) = (0, 0.2, 0)$. The set of initial conditions in Figure 4(b) leads to the chaotic attractor and a fixed point.

Electronic implementation of PMSMLT

The electronic implementation of PMSMLT on PSPICE software was done to verify the results found during the numerical simulations of PMSMLT. The advantages of electronic implementation include reduced costs and energy consumption, enhancing their performance and reliability. The electronic circuit diagram of the PMSMLT is given in Figure 5.

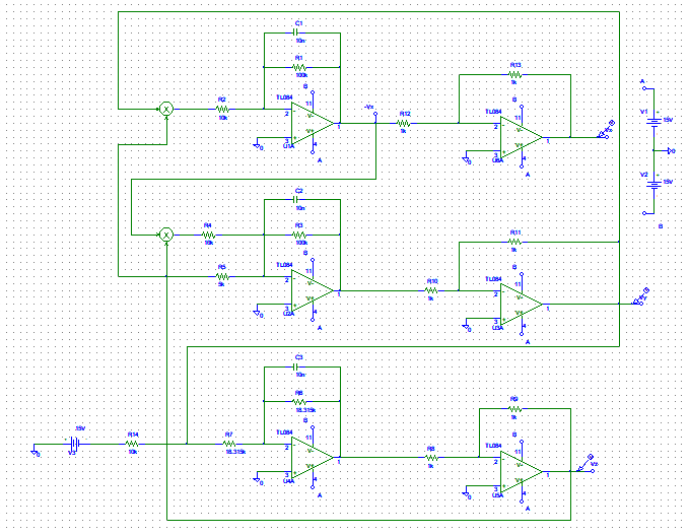

Figure 5 Circuit of the electronic implementation of the PMSMLT.

Figure 5 includes six operational amplifiers, two analog multipliers, three capacitors, fourteen resistors, a 15 V voltage source, and a symmetrical power supply of ±15 V. The phase portraits in Figure 6 are obtained from PSPICE.

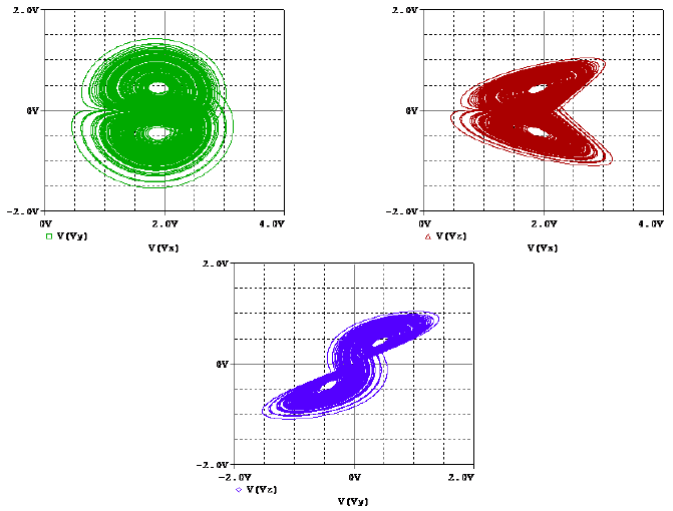

Figure 6 Phase portraits under PSPICE showing the chaotic behavior in the MSAP under load obtained for the resistance value $R_{14} = 10$ kΩ corresponding to the chaotic attractor. The other component values are $R_2 = R_4 = 10$ kΩ; $R_5 = 5$ kΩ; $R_1 = R_3 = 100$ kΩ; $R_8 = R_9 = R_{10} = R_{11} = R_{12} = R_{13} = 1$ kΩ; $R_6 = R_7 = 18.315$ kΩ, and $C_1 = C_2 = C_3 = 10$ nF. The initial conditions are $(IC_1, IC_2, IC_3) = (0.01, 0.01, 0.01)$.

The chaos encountered during the numerical simulations in Figures 2 (a) to (c) can be reproduced using electronic execution as shown in Figure 6.

CONTROL OF COEXISTING ATTRACTORS

Chaos and coexisting attractors encountered in PMSMLT are undesirable dynamical states in electrical machines. The linear augmentation control method is used to control the coexistence between chaos and no oscillations in PMSMLT (Sharma *et al.* 2015). The controlled system is written:

$$\frac{dx}{dt} = -x + yz, \tag{6a}$$

$$\frac{dy}{dt} = -y - xz + \gamma z, \tag{6b}$$

$$\frac{dz}{dt} = \sigma(y - z) + T_L, \tag{6c}$$

$$\frac{dv}{dt} = -\beta v - \delta(x - e), \tag{6d}$$

where Equation 6d is the control associated with the PMSMLT with β the decay parameter and δ the coupling parameter between the linear controller system and PMSMLT to be controlled. Figure 7 presents the superposition of the bifurcation diagrams obtained by control for the initial conditions having led to the coexistence between the chaos having the initial conditions $(x_0, y_0, z_0) = (0, 0, 0)$ and the fixed point having the initial conditions $(x_0, y_0, z_0) = (0, 0.2, 0)$.

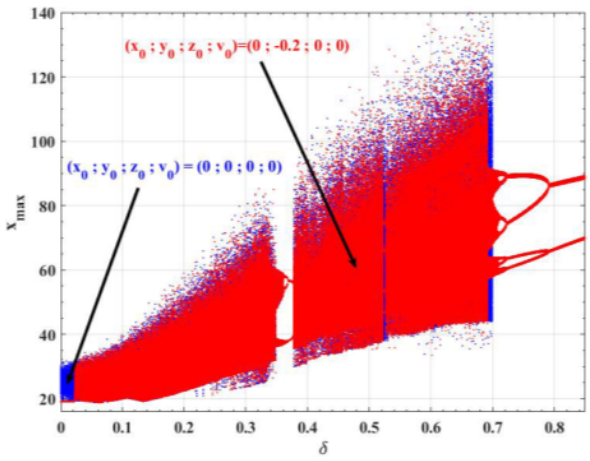

Figure 7 Bifurcation diagrams of x as a function of the coupling parameter δ of the controlled system obtained for the two initial conditions leading to multistability: $(x_0, y_0, z_0) = (0, 0, 0)$ for the color blue and $(x_0, y_0, z_0) = (0, 0.2, 0)$ for the color red. The parameter values are as follows: $\sigma = 5.46$, $\gamma = 20$, $T_L = 6.5$, $\beta = 0.01$, and $e = 5$.

In Figure 7, it reveals that when the coupling $\delta \leq 0.02$, the PMSMLT presents a coexistence of chaos and no oscillations. When this coupling force δ is adjusted in an increasing manner, the dynamics of the system tends towards monostability, corresponding to a limit cycle with two periods. Thus, Figure 7 shows the transition from multistability to monostability. In order to highlight the different transitions leading to the control of multistability in the PMSMLT, the phase portraits are made in Figure 8.

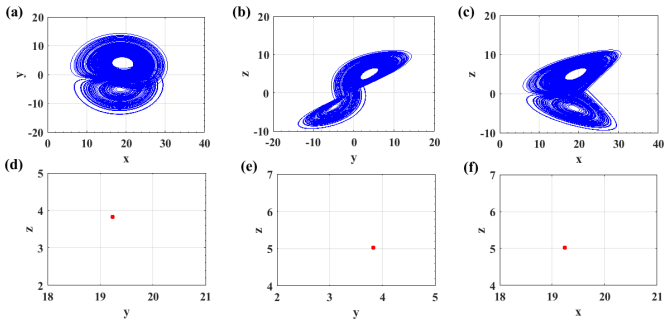

Figure 8 Phase portraits showing the coexistence of the fixed point and chaos obtained for $\sigma = 5.46$, $\gamma = 20$, $T_L = 6.5$, $\beta = 0.01$, $e = 5$, and $\delta = 0$. The lines in blue are obtained using the initial conditions $(x_0, y_0, z_0) = (0, 0, 0)$, while the lines in red are obtained using the initial conditions $(x_0, y_0, z_0) = (0, 0.2, 0)$.

For $\delta = 0$, the starting coexistence between chaos and no oscillations is illustrated in Figure 8. Figure 9 highlights the monostability of the PMSMLT by plotting the phase portraits.

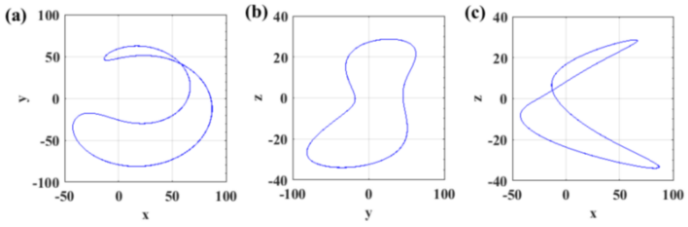

Figure 9 Phase portraits following the planes: (a) (x-y), (b) (y-z), and (c) (x-z) obtained for $\sigma = 5.46$, $\gamma = 20$, $T_L = 6.5$, $\beta = 0.01$, $e = 5$, and $\delta = 0.8$.

For $\delta = 0.8$, we observe monostability in the PMSMLT characterized by a two-period limit cycle illustrated by Figure 9.

CONCLUSION

The aim of this paper was to study the dynamics, electronic implementation, and control in permanent magnet synchronous motors with load torque (PMSMLT). PMSMLT presented no oscillations, periodic oscillations, chaos, and the coexistence between no oscillations and chaos, this for certain values of the load torque. The electronic implementation of the PMSMLT was carried out using the PSPICE software. The results obtained from the numerical simulations and the electronic implementation of the PMSMLT agree. The linear augmentation control method used made it possible to eliminate the coexistence between no oscillations and chaos in the PMSMLT. This paper helps in the field of electrical drives for industrial processes with variable speed and variable torque.

Availability of data and material

Not applicable.

Conflicts of interest

The authors declare that there is no conflict of interest regarding the publication of this paper.

Ethical standard

The authors have no relevant financial or non-financial interests to disclose.

LITERATURE CITED

Borisavljevic, A., 2013 *Limits, Modeling and Design of High-Speed Permanent Magnet Machines*. Springer.

Chapman, S. J., 2005 *Electric Machinery Fundamentals*. McGraw-Hill series in electrical and computer engineering, McGraw-Hill.

Chau, K. and Z. Wang, 2011 *Chaos in Electric Drive Systems: Analysis, Control and Application*. John Wiley and Sons.

Cheukem, A., A. S. Kemnang Tsafack, S. Takougang Kingni, C. C. André, and J. R. Mboupda Pone, 2020 Permanent magnet synchronous motor: chaos control using single controller, synchronization and circuit implementation. SN Applied Sciences **2**: 1–11.

Dong-lian, Q., J.-J. Wang, and Z. Guang-zhou, 2005 Passive control of Permanent Magnet Synchronous Motor chaotic systems. Journal of Zhejiang University SCIENCE **6**: 728–732.

Du-Qu, W. and Z. Bo, 2009 Controlling chaos in permanent magnet synchronous motor based on finite-time stability theory. Chinese Physics B **18**: 1399.

El-Sharkawi, M. A., 2000 *Fundamentals of Electric Drives*. Electrical Engineering Series, Brooks/Cole.

Fitzgerald, A. E., C. Kingsley, and S. Umans, 1991 *Electric Machinery*. Electrical Engineering Series, McGraw-Hill Companies,Incorporated.

Hua, C., Y. Wang, L. Zhang, and W. Ding, 2022 Stability and stabilization for the coupling permanent magnet synchronous motors system with input delay. Nonlinear Dynamics **107**: 3461–3471.

Hughes, A., 2006 *Electric Motors and Drives: Fundamentals, Types and Applications*. Electrical Engineering, Elsevier/Newnes.

Iqbal, A. and G. K. Singh, 2019 Chaos control of permanent magnet synchronous motor using simple controllers. Transactions of the Institute of Measurement and Control **41**: 2352–2364.

Leine, R. and H. Nijmeijer, 2004 *Dynamics and bifurcations of non-smooth mechanical systems*. Lecture notes in applied and computational mechanics, Springer, Germany.

Luo, S., 2014 Adaptive fuzzy dynamic surface control for the chaotic permanent magnet synchronous motor using Nussbaum gain. Chaos: An Interdisciplinary Journal of Nonlinear Science **24**: 33135.

Luo, S., J. Wang, Z. Shi, and Q. Qiu, 2014 Output Feedback Adaptive Dynamic Surface Control of Permanent Magnet Synchronous Motor with Uncertain Time Delays via RBFNN. Discrete Dynamics in Nature and Society **2014**: 315634.

Machowski, J., J. W. Bialek, and J. R. Bumby, 2012 Power System Dynamics. Stability and Control. John Wiley and Sons .

Maeng, G. and H. H. Choi, 2013 Adaptive sliding mode control of a chaotic nonsmooth-air-gap permanent magnet synchronous motor with uncertainties. Nonlinear Dynamics **74**: 571–580.

Mao, W.-L. and G.-Y. Liu, 2019 Development of an Adaptive Fuzzy Sliding Mode Trajectory Control Strategy for Two-axis PMSM-Driven Stage Application. International Journal of Fuzzy Systems **21**: 793–808.

Santoso, S. and H. W. Beaty, editors, 2018 *Standard Handbook for Electrical Engineers*. McGraw-Hill Education, New York, 17th edition.

Say, M. G. and E. O. Taylor, 1980 Direct current machines. (No Title) .

Sharma, P. R., M. D. Shrimali, A. Prasad, N. V. Kuznetsov, and G. A. Leonov, 2015 Control of multistability in hidden attractors. The European Physical Journal Special Topics **224**: 1485–1491.

Vadivel, R., Z. T. Njitacke, L. Shanmugam, P. Hammachukiattikul, and N. Gunasekaran, 2023 Dynamical analysis and reachable set estimation of t-s fuzzy system with permanent magnet syn-

chronous motor. Communications in Nonlinear Science and Numerical Simulation **125**: 107407.
Wildi, T., 2006 *Electrical Machines, Drives, and Power Systems*. Pearson Prentice Hall, fifth edition.
Yamdjeu, G., B. Sriram, S. T. Kingni, K. Rajagopal, and A. Mohamadou, 2024 Analysis, microcontroller implementation and chaos control of non-smooth air-gap permanent magnet synchronous motor. Pramana - Journal of Physics **98**: 126.

How to cite this article: Fotsa, R. T., Papemsi, P. K., Kuete, G. P. A., Pone, J. R. M., Naoussi, S. R. D., Momo, F., and Ele, P. Permanent Magnet Synchronous Motor with Load Torque: Dynamics, Circuitry Execution and Control. *Chaos and Fractals*, 2(1), 14-19, 2025.